Supplementary Information

First-principles study on structural stabilities, mechanical properties, and biaxial strain-induced superconductivity in Janus MoWC monolayer

Sirinee Thasitha,[a] Prutthipong Tsuppayakorn-aek,[b,g] Anan Udomkijmongkol,[a] Satchakorn Khammuang,[a] Thanayut Kaewmaraya,[c,d] Tanveer Hussain,[e,f] Thiti Bovornratanaraks,[b,g] Komsilp Kotmool[a,*]

[a]College of Advanced Manufacturing Innovation, King Mongkut's Institute of Technology Ladkrabang, Bangkok 10520, Thailand. E-mail: komsilp.ko@kmitl.ac.th; Tel: +66 2329 8264

[b]Extreme Conditions Physics Research Laboratory and Center of Excellence in Physics of Energy Materials (CE:PEM), Department of Physics, Faculty of Science, Chulalongkorn University, Bangkok 10330, Thailand

[c]Integrated Nanotechnology Research Center, Department of Physics, Khon Kaen University, Khon Kaen, Thailand

[d]Institute of Nanomaterials Research and Innovation for Energy (IN-RIE), NANOTEC-KKU RNN on Nanomaterials Research and Innovation for Energy, Khon Kaen University, Khon Kaen, 40002, Thailand

[e]School of Chemical Engineering, The University of Queensland, St Lucia, Brisbane, 4072, Australia

[f]School of Science and Technology, University of New England, Armidale, New South Wales 2351, Australia

[g]Thailand Center of Excellence in Physics, Ministry of Higher Education, Science, Research and Innovation, 328 Si Ayutthaya Road, Bangkok, 10400, Thailand

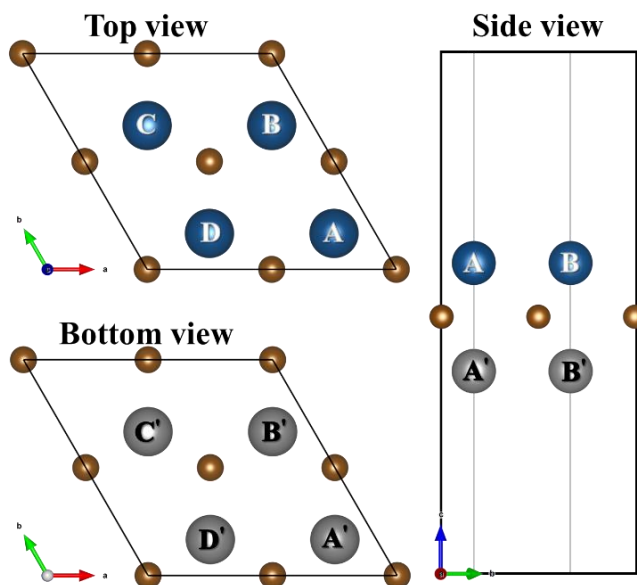*Corresponding E-mail: komsilp.ko@kmitl.ac.th

Fig. S1 Top, bottom, and side views of the 2H-MoWC within the 2×2×1 supercell.

Table S1 The atomic arrangement of the 2H-MoWC phase in each model respecting the atomic positions in Fig. S1.

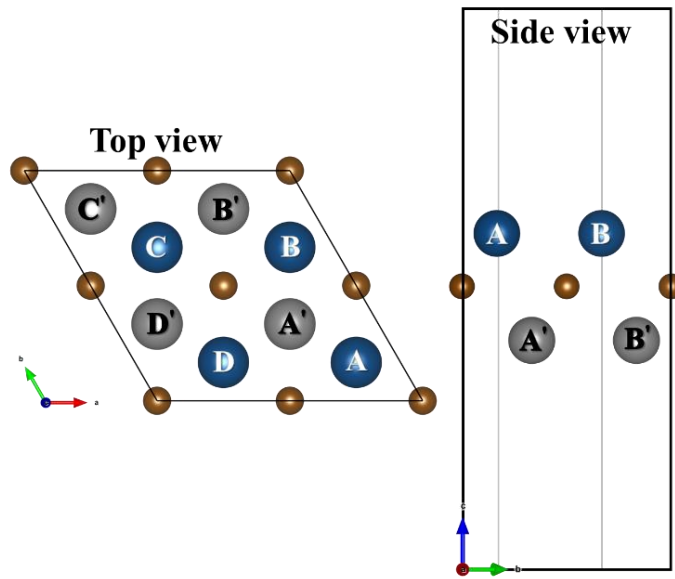| Model	Positions							
	A	B	C	D	A$'$	B$'$	C$'$	D$'$
2H-MoWC-I	Mo	Mo	Mo	Mo	W	W	W	W
2H-MoWC-II	W	Mo	Mo	Mo	Mo	W	W	W
2H-MoWC-III	W	Mo	W	Mo	Mo	W	Mo	W
2H-MoWC-IV	Mo	Mo	W	W	W	W	Mo	Mo
2H-MoWC-V	W	Mo	W	Mo	W	Mo	W	Mo
2H-MoWC-VI	Mo	Mo	W	Mo	W	Mo	W	W
2H-MoWC-VII	Mo	Mo	W	W	Mo	Mo	W	W
2H-MoWC-VIII	Mo	Mo	Mo	W	W	Mo	W	W
2H-MoWC-IX	Mo	Mo	W	W	Mo	W	Mo	W
2H-MoWC-X	W	Mo	W	Mo	W	W	Mo	Mo

Fig. S2 Top, bottom, and side views of the 1T-MoWC within the 2×2×1 supercell.

Table S2 The atomic arrangement of the 1T-MoWC phase in each model from the atomic positions depicted in Fig. S2.

Model	Positions							
	A	**B**	**C**	**D**	**A'**	**B'**	**C'**	**D'**
1T-MoWC-I	Mo	Mo	Mo	Mo	W	W	W	W
1T-MoWC-II	W	Mo	Mo	Mo	Mo	W	W	W
1T-MoWC-III	W	Mo	W	Mo	Mo	W	Mo	W
1T-MoWC-IV	Mo	Mo	W	W	W	W	Mo	Mo
1T-MoWC-V	W	Mo	W	Mo	W	Mo	W	Mo
1T-MoWC-VI	Mo	Mo	W	Mo	W	Mo	W	W
1T-MoWC-VII	Mo	Mo	W	W	Mo	Mo	W	W
1T-MoWC-VIII	Mo	Mo	Mo	W	W	Mo	W	W
1T-MoWC-IX	Mo	Mo	W	W	Mo	W	Mo	W
1T-MoWC-X	Mo	W	Mo	W	Mo	W	W	Mo

Table S3 Lattice parameter a, b, c (Å), angle α, β, γ (deg.), relative energies (ΔE) in meV/ f.u. (f.u. stands for formula unit) respecting the lowest one of all calculated configurations of the 2H- and 1T-MoWC phases without spin-orbit coupling.

| Phase | Lattice parameter (Å) | | | Angle (deg.) | | ΔE |
	a	b	α	β	γ	(meV/f.u.)
2H-MoWC-I	5.678	5.678	89.986	90.014	119.909	0
2H-MoWC-II	5.677	5.677	89.993	90.007	119.921	6
2H-MoWC-III	5.676	5.676	90.000	90.000	119.901	8
2H-MoWC-IV	5.677	5.676	90.000	90.000	119.908	8
2H-MoWC-V	5.676	5.676	90.000	90.000	119.929	15
2H-MoWC-VI	5.677	5.678	89.993	90.006	119.925	10
2H-MoWC-VII	5.676	5.679	90.000	90.000	119.940	15
2H-MoWC-VIII	5.677	5.677	89.995	90.005	119.923	10
2H-MoWC-IX	5.676	5.677	89.999	90.001	119.927	12
2H-MoWC-X	5.676	5.677	89.998	90.004	119.924	12
1T-MoWC-I	5.848	5.848	90.061	89.939	120.052	335
1T-MoWC-II	5.841	5.841	90.038	89.962	120.046	330
1T-MoWC-III	5.816	5.816	89.985	90.015	120.030	334
1T-MoWC-IV	5.844	5.842	90.054	89.974	120.043	326
1T-MoWC-V	5.853	5.853	90.082	89.918	120.056	321
1T-MoWC-VI	5.844	5.845	90.054	89.918	120.058	327
1T-MoWC-VII	5.826	5.829	90.036	89.909	120.059	327
1T-MoWC-VIII	5.834	5.834	90.054	89.946	120.055	331
1T-MoWC-IX	5.834	5.835	90.037	89.952	120.049	326
1T-MoWC-X	5.837	5.837	90.053	89.958	120.050	327

Table S4 Lattice parameter a, b, c (Å), angle α, β, γ (deg), relative energies (ΔE) in meV/ f.u. (f.u. stands for formula unit) respecting the lowest one (2H-MoWC-I) of all calculated configurations of the 2H- and 1T-MoWC phases with spin-orbit coupling.

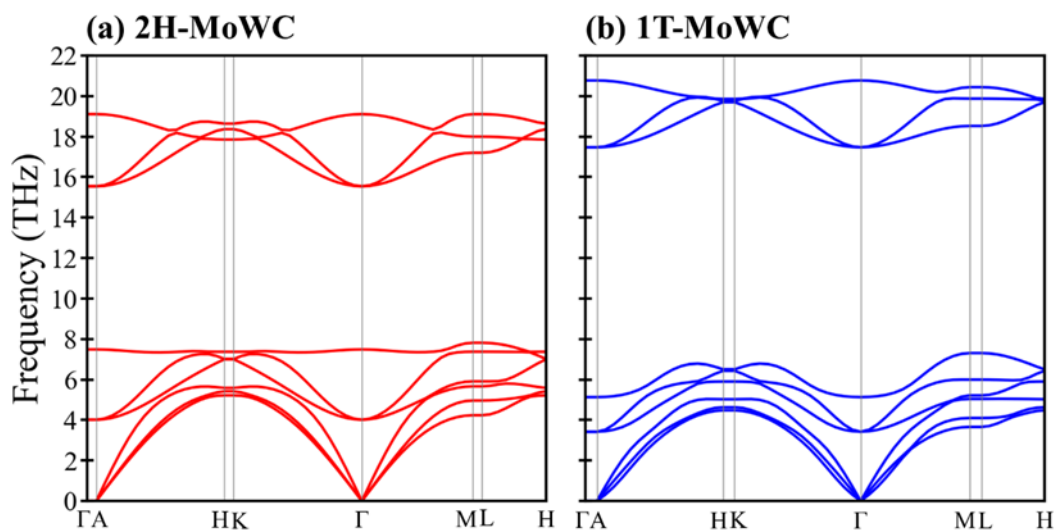| Phase | Lattice parameter (Å) | | | Angle (deg.) | | ΔE |
	a	b	α	β	γ	(meV/f.u.)
2H-MoWC-I	5.687	5.687	90.000	90.000	120.000	0
2H-MoWC-II	5.685	5.685	90.000	90.000	120.000	7
2H-MoWC-III	5.685	5.685	90.001	89.999	120.034	9
2H-MoWC-IV	5.686	5.683	90.000	90.000	119.983	9
2H-MoWC-V	5.687	5.687	90.000	90.000	120.087	15
2H-MoWC-VI	5.687	5.684	90.002	90.000	120.023	9
2H-MoWC-VII	5.687	5.679	90.000	90.000	119.957	15
2H-MoWC-VIII	5.684	5.684	90.000	90.001	119.956	9
2H-MoWC-IX	5.687	5.684	88.371	93.386	120.021	11
2H-MoWC-X	5.687	5.683	90.095	89.800	120.023	12
1T-MoWC-I	5.848	5.848	90.061	89.939	120.052	386
1T-MoWC-II	5.841	5.841	90.038	89.962	120.046	387
1T-MoWC-III	5.816	5.816	89.985	90.015	120.030	392
1T-MoWC-IV	5.844	5.842	90.054	89.974	120.043	386
1T-MoWC-V	5.792	5.792	89.608	90.381	119.926	380
1T-MoWC-VI	5.802	5.803	90.008	90.128	120.009	401
1T-MoWC-VII	5.827	5.829	90.036	89.909	120.059	389
1T-MoWC-VIII	5.834	5.834	90.054	89.946	120.055	393
1T-MoWC-IX	5.798	5.801	89.853	90.009	119.985	383
1T-MoWC-X	5.837	5.837	90.053	89.958	120.050	387

Fig. S3 The phonon dispersion curves of the 2H (a) and 1T (b) phases of the Janus MoWC monolayer at unstressed conditions show that these two phases are dynamically stable, as there are no imaginary phonon frequencies present.
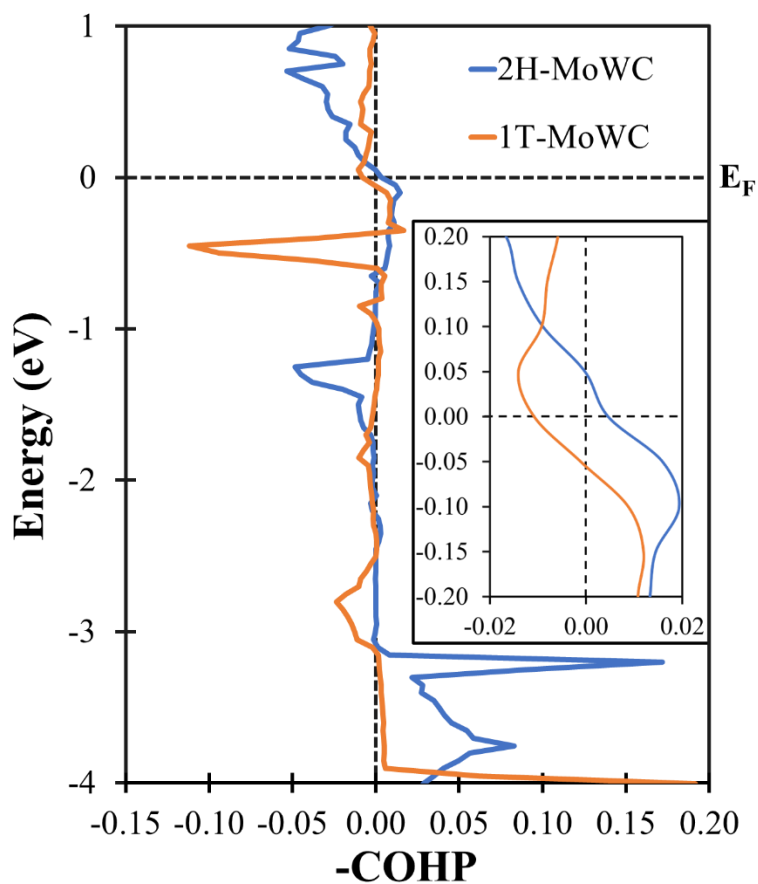

Fig. S4 The COHP plot of the C-C bond in both the 2H and 1T phases.

Table S5 The elastic constants (C_{ij} values) for the 2H and 1T-MoWC phases.

Model	Elastic constants (GPa)						Ref.
	$C_{11} = C_{22}$	C_{12}	C_{13}	C_{33}	C_{44}	$C_{55} = C_{66}$	
2H-MoWC-I	561	241	137	455	160	137	This work
1T-MoWC-I	539	156	236	178	191	88	This work
Ti_3C_2	422	132	133	295	145	150	This work
Ti_3C_2	473						[1]

To bolster reliability, we replicated the calculated elastic constant in our study. Furthermore, we computed the elastic constant for Ti_3C_2 MXene material to juxtapose against existing data, as detailed in Table S5. Our findings demonstrate that our methodology produced elastic constants for Ti_3C_2 consistent with those reported previously. Hence, we have confidence in the reliability of the reproduced elastic constant for the Janus MoWC monolayer.

References

[1]   N. Zhang, Y. Hong, S. Yazdanparast, and M. A. Zaeem, "Superior structural, elastic and electronic properties of 2D titanium nitride MXenes over carbide MXenes: a comprehensive first principles study," *2D Materials,* vol. 5, no. 4, p. 045004, 2018.